Anisotropy in surface resistivity due to electron-phonon scattering in aluminium

1994 J. Phys.: Condens. Matter 6 9585

(http://iopscience.iop.org/0953-8984/6/45/009)

J. Phys.: Condens. Matter 6 (1994) 9585–9600. Printed in the UK

Anisotropy in surface resistivity due to electron–phonon scattering in aluminium

Isao Nakamichi

Cryogenic Centre and Faculty of Science, Hiroshima University, Higashi-Hiroshima 724, Japan

Received 1 July 1994

Abstract. The electrical resistivity ρ has been measured at temperatures from 1.5 to 75 K for two series of foils with {111} and {110} surfaces on zone-refined Al, under the same current direction of ⟨112⟩. It is found that ρ is larger on the {111} foil than the {110} one at 1.5–60 K and their difference peaks at around 35 K. The analysis of the data with Fuchs–Sondheimer theory gives the following results. (i) The phonon-limited part of the bulk-electron mean free path, $l_b(T)$, is larger along about ⟨111⟩ ($l_b^{111}(T)$) than the orientations around ⟨110⟩ ($l_b^{110}(T)$), and agrees with the value from the electron–phonon scattering time calculated by Leung *et al* at 20 K. (ii) $l_b^{111}(T)$ varies as $T^{-3.0}$, but $l_b^{110}(T)$ varies as $T^{-3.5}$ at 10–20 K; this is consistent with Meador and Lawrence's theoretical prediction. The surface resistivity ρ_s of the single crystals is about half of that of the polycrystal of pure Al. It is concluded that the enhancement of ρ_s due to anisotropy in $l_b(T)$ is the main cause of the discrepancies between the measured and predicted ρ_s in polycrystals.

1. Introduction

Size effects in electrical resistivity have been of considerable interest. The foil resistivities measured are well explained by the classical theory of Fuchs (1938) and Sondheimer (1952) (FS theory) on their thickness dependence. However, the surface resistivity ρ_s strongly depends on temperature, causing deviation from Matthiessen's rule for ρ_s. It become larger than that estimated from FS theory, as reviewed by Bass (1972). Sambles and Elson (1980) have explained this discrepancy, using Soffer's (1967) surface-reflection parameter, which depends on the electron incidence angle (Soffer's theory). This explanation, however, was later doubted by themselves, because these theories are based on the isotropic relaxation time and Al has a rather complicated Fermi surface (Sambles and Mundy 1983).

Recently, the present author has found that the nature of bulk scattering has a great effect on ρ_s. Instead of temperature, we have varied the concentration of Ag in dilute Al–Ag polycrystalline foils at 4.2 K to vary the bulk mean free path l_b. ρ_s of the solid solution of Al–Ag at 4.2 K has been shown to be smaller than that of pure Al at tens of kelvin, in good agreement with FS theory (Nakamichi and Kino 1988). In addition, in the more concentrated Al–Ag alloys with Guinier–Preston (GP) zones, the ρ_s at 4.2 K becomes four to five times larger than that of the Al–Ag solid solution (Nakamichi 1989). These results are consistent with the theoretical prediction of Bate *et al* (1963) that the anisotropy in mean free path enhances ρ_s in polycrystals, because the GP zone has a strongly anisotropic scattering in contrast to the fairly isotropic scattering of the Al–Ag solid solution. These results suggest that the discrepancy between measured and calculated ρ_s at low temperatures arises from the anisotropy in electron–phonon scattering (Nakamichi and Kino 1988).

0953-8984/94/459585+16$19.50

The aim of the present experiment is to detect the anisotropy in ρ_s due to electron–phonon scattering in Al in confirmation of the above suggestion. The temperature-dependent anisotropy in ρ_s has been investigated previously in Al (Risnes and Sollien 1969, Risnes 1970). However, the temperature range measured was limited to 2–15 K and neither the crystallographic orientations nor the purity (bulk resistivity ρ_b) of crystals seem to be well controlled. The present experiment has been performed over the wide range of 1.5–75 K, using single crystals controlled well in both orientation and purity. For the foil surface, {111} and {110} planes have been chosen, because the phonon-limited part of l_b, $l_b(T)$ is the longest along ⟨111⟩ in Al and is an order of magnitude larger than along ⟨110⟩, according to the theoretical calculations (Leung *et al* 1976, 1977). That is, we will find that ρ_s is larger on {111} than {110}, because the numbers of electrons reaching the specimen surface increase as l_b increases.

Also this experiment will give information on the anisotropy in electron–phonon scattering. Such information has been reported from the surface-Landau-level-resonance (Wegehaupt and Doezema 1978), radio-frequency-size-effect (Parsons and Steele 1979) and Sondheimer-size-effect measurements on Al (Sato 1980). However, no resistivity measurements in zero magnetic field seem to have been clearly given yet.

In this paper, first, experimental details and results are described in sections 2 and 3. In section 4, the theoretical background is described; in particular, the effect of anisotropic l_b on the analysis with FS theory is described in detail, in addition, it is checked whether the anisotropy in ρ_s arises from that in the surface-reflection parameter or l_b. In section 5, the results are analysed with FS theory in detail; they are discussed and compared with the other theories and experiments related to the scattering anisotropy.

2. Experimental details

Two sets of strips with (111) and $(\bar{1}10)$ surfaces were prepared by spark erosion from a single crystalline block of zone-refined Al with a bulk residual resistance ratio (RRR) of 15 000. Both sets of strips are 0.8 and 0.5 mm in thickness and 3 mm in width, and have the lengthwise (current) direction of $[\bar{1}\bar{1}2]$. Specimen surface layers of a few micrometres thickness were etched off with a chemical solution of $70H_3PO_4 + 25H_2SO_4 + 5HNO_3$ to remove those contaminated during the spark erosion. The chemical solution was washed away with hot distilled water. The specimens were annealed at 573 K for 1 h in air after spot-welding pure Al leads; this annealing condition was chosen as it gave the highest RRR value; the rather-low-temperature anneal can avoid contamination during the anneal. After the first resistivity measurement, the strips ({111} and {110}) with 0.5 mm thickness were further thinned by spark erosion using a rotary electrode. They were etched, annealed as above and this was followed by the second resistivity measurement. Further, they were thinned, etched and annealed, followed by the third resistivity measurement.

The cryostat for the resistivity measurement has a specimen chamber of double-wall cans, of which the inner one was filled with He gas above 4.2 K. Below 4.2 K, the specimens were directly immersed in the liquid He. The temperatures were controlled within 0.01 K below 4.2 K and within 0.05 K above 4.2 K, and were measured with a calibrated Allen–Bradley C resistor and an Au–Co thermocouple. The reproducibilities of the thermometers were checked at 4.2 K on each measurement. A pair of foils with {111} and {110}, with nearly the same thickness, was mounted on the Al specimen holder coated with a thin film for electrical insulation, and their resistances were measured simultaneously.

The electrical resistivity of foils with thickness d at a temperature T, $\rho(d, T)$ was calculated from the measured resistances of the specimen, $R(T)$ at T and $R(300\ \mathrm{K})$ at 300 K, by

$$\rho(d, T) = 2.733\ \mathrm{n\Omega\ m}\ R(T)/R(300\ \mathrm{K}) \tag{1}$$

where 2.733 nΩ m is the bulk resistivity at 300 K (Kawata and Kino 1975). These electrical resistances were measured with an Otto Wolff KDE 84 potentiometer having a sensitivity of 3 nV. The resistance $R(300\ \mathrm{K})$ was measured in an oil bath regulated at 300 ± 0.01 K. This gives the specimen size factor, which determines the relative error of ρ, within $\pm 0.01\%$. The specimen thickness d was determined from $\rho(300\ \mathrm{K}) = 2.733\ \mathrm{n\Omega\ m}$, $R(300\ \mathrm{K})$, and the width and length measured with a travelling microscope. To take into account the limited specimen width, the reduced thickness d_r, defined as $d_r = 2 \times$ (cross-section/perimeter), is introduced (Dingle 1950). The specimen dimensions are listed in table 1, together with the residual resistivity.

Table 1. The specimen dimensions and residual resistivity $\rho(1.5\ \mathrm{K})$. d_r is the reduced thickness.

Surface plane	Thickness (μm)	Width (mm)	d_r (μm)	$\rho(1.5\ \mathrm{K})$ (pΩ m)
{110}	774	2.88	610	2.22
	459	2.93	397	2.63
	254	2.88	234	3.10
	173	2.79	163	3.20
{111}	843	2.73	644	2.30
	549	2.91	462	2.72
	316	2.85	285	2.91
	181	2.68	169	3.26

3. Results

Figures 1 and 2 are the resistivity ρ plotted against temperature T for four thicknesses and for {111} and {110} foils below 20 K; the current direction ⟨112⟩ is the same on both foils and is omitted below. Figure 3 is ρ plotted against $1/d_r$ for four temperatures, typically. This shows that, when the thicknesses are equal, ρ^{111} is larger than ρ^{110} in this temperature range, where ρ^{111} and ρ^{110} are the resistivities for foils with {111} and {110} planes, respectively. The difference between ρ^{111} and ρ^{110} increases with decreasing thickness.

Figure 4 is the value of $\rho^{111} - \rho^{110}$ plotted against T up to 75 K for two pairs of foils. $\rho^{111} - \rho^{110}$ is equal to the difference of surface resistivity ρ_s between the foil with {111} and that with {110}, because

$$\rho = \rho_b + \rho_s \tag{2}$$

and the bulk resistivity ρ_b is the same in both foils. The resistivity difference between the foils of 169 and 163 μm thickness increases with temperature, maximizing at around 35 K, and tends to be negative above about 60 K; the small peak at around 19 K originates from the difference in the temperature of the ρ_s peak between {111} and {110} foils, as will be

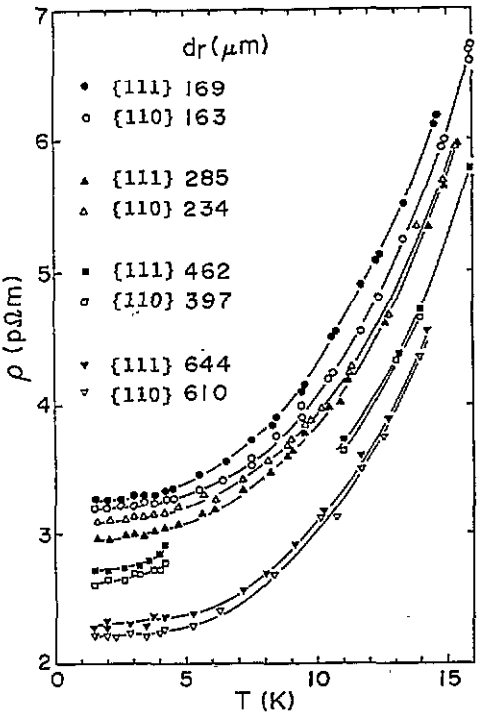

Figure 1. The electrical resistivity ρ from 1.5 to 16 K for four foil thickness pairs. Each pair has nearly the same thickness but different surface planes of {111} and {110} as shown in the figure, where d_r is the reduced thickness.

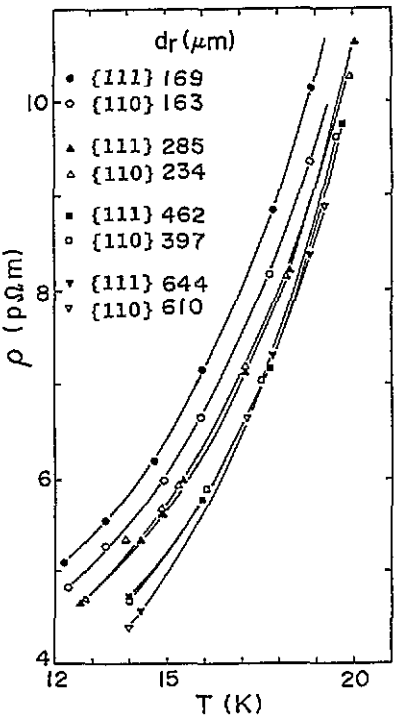

Figure 2. The same plot as figure 1 for the higher temperature range of 12–20 K.

seen in figure 5(*a*). In the thicker foil pair (285 and 234 μm), $\rho^{111} - \rho^{110}$ is slightly negative at low temperature, but it also becomes positive above 19 K and maximizes at around the same temperature of 35 K. The negative values of $\rho^{111} - \rho^{110}$ below 19 K are attributed to the fact that the {110} specimen is thinner than {111} specimen (by about 20%) in this case. This can be confirmed by figure 3; at the same thickness, ρ^{111} is larger than ρ^{110} even below 19 K. Thus, these two curves show that ρ_s^{111} is larger than ρ_s^{110} below about 60 K and their difference is largest at around 35 K.

To examine the effect of electron–phonon scattering on ρ_s in more detail, we make a logarithmic plot of the temperature-dependent part of ρ_s, $\rho_s(T)$, against T for three specimens with nearly the same thickness in figure 5(*a*). For comparison, the data for a polycrystalline foil of zone-refined Al (Nakamichi and Kino 1980) are also included. The use of $\rho_s(T)$, instead of ρ_s, has the advantage that it is independent of both the impurities and lattice defects that might be introduced into thin foils during the heating and handling processes. $\rho_s(T)$ is obtained as $(\rho - \rho(1.5\ \mathrm{K})) - (\rho_b - \rho_b(1.5\ \mathrm{K}))$, where $\rho(1.5\ \mathrm{K})$ and $\rho_b(1.5\ \mathrm{K})$ are the resistivities at 1.5 K for foils and bulk specimen, respectively. Here, ρ of the thickest specimen with 0.8 mm thickness is used as ρ_b, because ρ_s of the thickest specimen hardly depends on the temperature (Nakamichi and Kino 1980). $\rho_b(T)$ is shown in figure 5(*b*).

Figure 5(*a*) clearly shows that $\rho_s^{poly}(T) > \rho_s^{111}(T) > \rho_s^{110}(T)$; where $\rho_s^{poly}(T)$, $\rho_s^{111}(T)$ and $\rho_s^{110}(T)$ are the $\rho_s(T)$ values for polycrystalline, {111} and {110} foils, respectively.

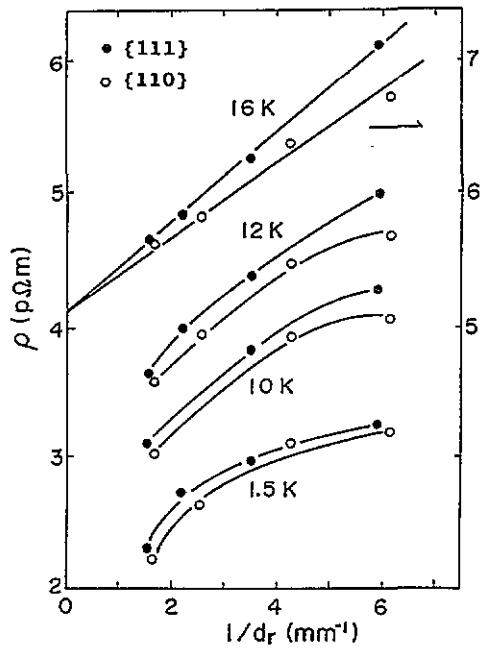

Figure 3. The resistivity ρ against the inverse of reduced thickness d_r for four temperatures typically.

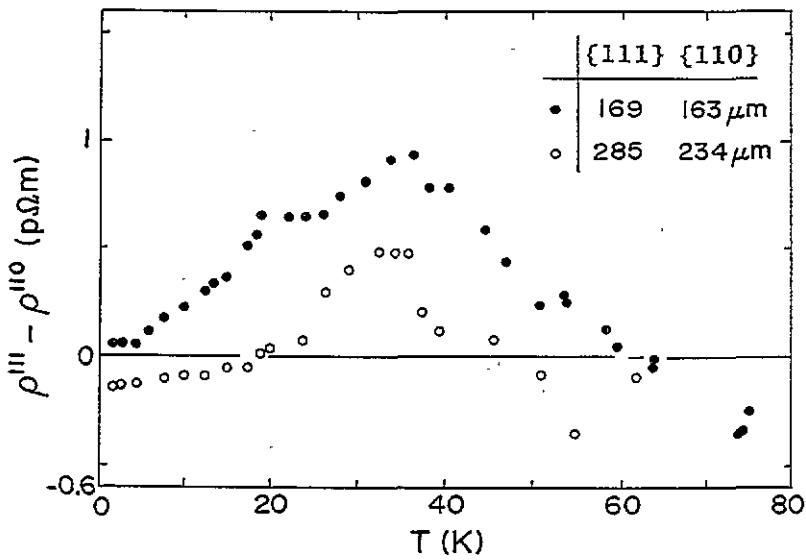

Figure 4. The variation of the difference between the resistivity ρ^{111} of {111} foils and ρ^{110} of {110} ones for two pairs at 1.5–75 K.

It should be noted that $\rho_s(T)$ in polycrystals is about two and six times larger than that in single crystals with {111} and {110} surfaces, respectively, in this temperature range. $\rho_s(T)$ shows T^2 dependence in a certain temperature range. Figure 5(*b*) shows that $\rho_b(T)$ depends

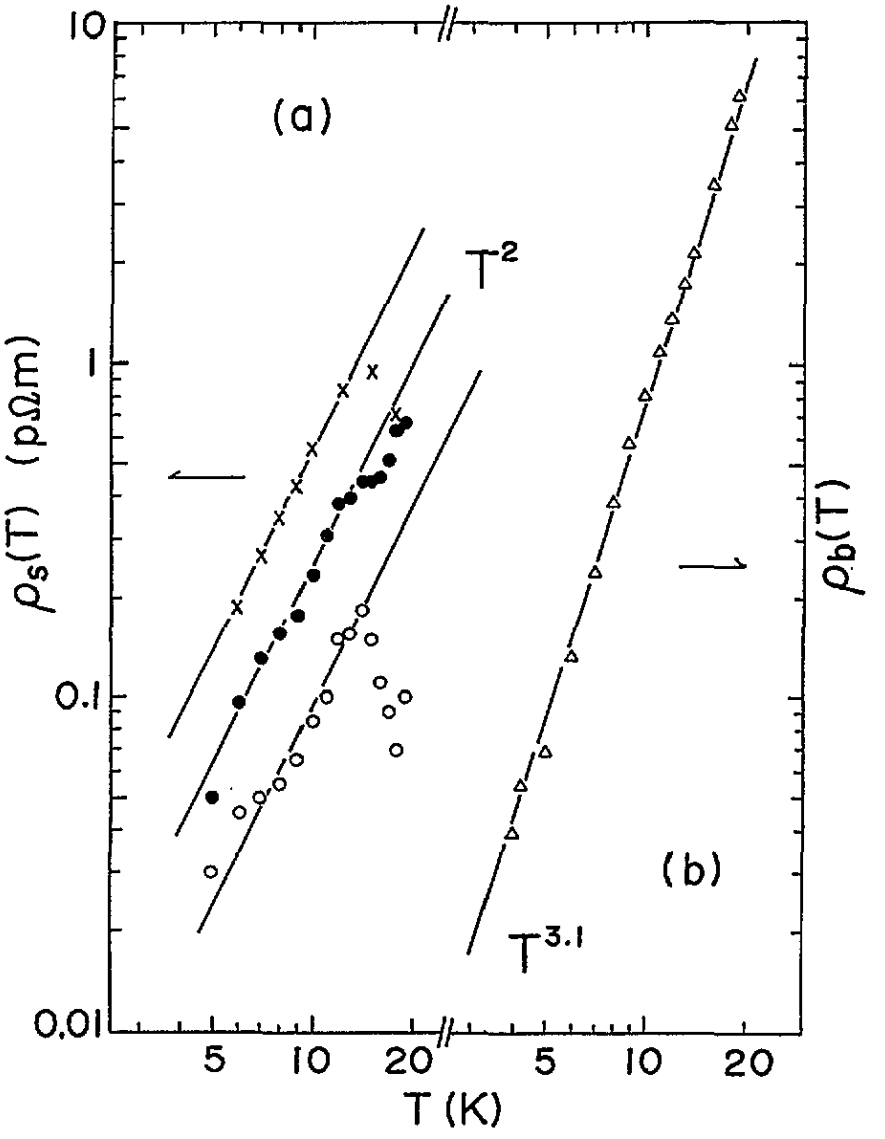

Figure 5. (*a*) A logarithmic plot of the temperature-dependent part of the surface resistivity $\rho_s(T)$ against T for polycrystalline and single-crystal foils with nearly the same thicknesses. ×, a polycrystalline foil of 184 μm thickness; ●, a {111} foil of 169 μm; ○, a {110} foil of 163 μm. (*b*) The same plot for the bulk resistivity $\rho_b(T)$. $\rho_s(T)$ is obtained as $(\rho - \rho(1.5\ \mathrm{K})) - (\rho_b - \rho_b(1.5\ \mathrm{K}))$. For ρ_b, ρ of the specimen with 0.8 mm thickness is used.

on $T^{3.1}$ at 4–19 K; this becomes a nearly T^5 dependence at higher temperatures, which is not shown here. The T^2 dependence of $\rho_s(T)$ has been predicted by Sambles and Preist (1982) when $\rho_b(T)$ depends on T^2 or T^5. However, figure 5 shows that it occurs even if $\rho_b(T)$ depends on $T^{3.1}$. In addition, the temperature range of T^2 dependence of $\rho_s(T)$ is rather limited, but this suggests that we have to be careful not to confuse the surface scattering and the electron–electron scattering on the T^2 contribution to resistivity.

4. Theoretical background and pre-analysis

4.1. FS and Soffer's theories

Fuchs and Sondheimer have shown, assuming isotropic bulk scattering, that the resistivity ρ for a thin foil with thickness d is expressed as (FS theory)

$$\rho/\rho_b = F(\kappa, p) = \left[1 - \frac{3(1-p)}{2\kappa}\int_1^\infty \left(\frac{1}{t^3} - \frac{1}{t^5}\right)\frac{1-e^{-\kappa t}}{1-pe^{-\kappa t}}\,dt\right]^{-1} \tag{3}$$

where p is the specularity parameter, defined as the fraction of specular scattering at the surface, and $\kappa = d/l_b$. When $l_b \ll d$, the theory becomes

$$\rho = \rho_b[1 + \tfrac{3}{8}(1-p)l_b/d]. \tag{4}$$

More practically, when $l_b < 2d_r$, Kirkland and Chaplin (1971) have shown that FS theory is approximated as

$$\rho = \rho_b[1 + 0.46(1-p)l_b/d_r]. \tag{5}$$

As for the surface resistivity ρ_s, it is expressed with the $F(\kappa, p)$ as

$$\rho_s = (\rho_b l_b/d)\kappa(F(\kappa, p) - 1). \tag{6}$$

In contrast to FS theory, Soffer (1967) has considered the specularity parameter as depending on both the electron incidence angle and the surface roughness r (referred to as p_s). Soffer's theory, however, has the same form as equation (3) except that p_s replaces p.

4.2. The origin of observed anisotropy in ρ_s: pre-analysis

There are two possibilities for the origin of the anisotropic ρ_s observed. One is the anisotropy in specularity parameter, and the other is the anisotropy in l_b. The former is checked as follows. Both FS and Soffer's theories predict that ρ_s is nearly a constant, which depends on p or r, when $d/l_b > 20$ (at high T) (Sambles and Elson 1980), we see that equation (4) also predicts that $\rho_s = (3/8d)\ (1-p)\rho_b l_b$ =constant when $l_b \ll d$. This leads to the prediction that $\rho^{111} - \rho^{110}$ should become almost constant when $d/l_b > 20$, if the orientation dependence of ρ_s arises from the difference in the specularity parameter. At 40 K, l_b is about 70 μm in zone-refined Al (Nakamichi and Kino 1980) and the condition $d/l_b > 20$ is satisfied above 40 K for the foils in the present work. However, as seen in figure 4, $\rho^{111} - \rho^{110}$ does not become constant, decreasing monotonically with T above 40 K. This shows that the difference in ρ_s between {111} and {110} foils does not arise from the difference in the specularity parameter.

In this work, we take $p = 0$ (a rough limit on Soffer's theory) following the previous experimental determination on polycrystalline Al (Nakamichi and Kino 1980); Soffer's theory agrees with FS theory in the rough limit (Sambles and Elson 1980). This choice is realistic because the etching should have made the height of surface roughness much larger than the electron wavelength in the present experiment.

Thus, the anisotropy in ρ_s must arise from the anisotropy in l_b. This can be confirmed by using equation (5) and the data at 16 K in figure 3, which satisfy the condition $l_b < 2d_r$. The two sets of data lie well on the respective lines. Comparing these lines with equation (5), we see that the intersection at $1/d_r = 0$ is ρ_b and the slopes are the product $\rho_b l_b$. Since ρ_b is the same in the two series of foils, the larger slope of the data for {111} foils shows that not only $\rho_b l_b$ but also l_b is larger in the {111} foil than the {110} one. The meaning of this will be described in more detail in the following section.

4.3. The mean free path l_b: the meaning of the application of FS theory

Usually, the values of ρ_b and l_b are obtained by the fitting of the experimental data to FS theory, varying ρ_b and l_b. As seen from equation (5), this fitting gives a larger value of l_b with increasing ρ when ρ_b is fixed. This is reasonable because the longer l_b is, the more electrons reach the surface, increasing ρ_s. However, it is necessary to consider the meaning of the application of FS theory to the case of anisotropic l_b, because the theory regards l_b as isotropic originally. In other words, FS theory considers that the electrons for any direction have the same l_b as the electrons reaching the surface. This problem is checked using the more general Chambers' equation as follows.

For the case of anisotropic l_b, Chambers (1969) has given the following conductivity $\sigma_{ij}(r)$, which depends on the position r within a metal:

$$\sigma_{ij}(r) = (e^2/4\pi^3\hbar) \int dS_F (n_i n_j l_b)^k (1 - \exp(-d_s/l_b^k)) \tag{7}$$

where S_F is the Fermi surface, n_i is a component (along the i direction) of the unit vector normal to S_F at point k, and d_s is the path length travelled by an electron with a wave vector k from the position r to the metal surface. The integration is over the Fermi surface. When l_b is isotropic, this leads to the same form as the FS theory. The equation (7) is difficult to use directly for the analysis of experimental data without the precise knowledge of k dependence of l_b^k. However, it gives the meaning of the anisotropic l_b obtained from the analysis with FS theory.

The term $\exp(-d_s/l_d^k)$ reduces the conductivity. Thus, ρ_s arises from the sum of this term over the electrons that travel towards the sample surface and have the component along the current direction. Since the exponential term increases as d_s decreases or as l_b^k increases, ρ_s is mainly caused by the electrons travelling nearly vertically to the sample surface, if l_b is much longer along the surface normal than the surrounding orientations. In this case, the fitting of the experimental data to FS theory gives l_b nearly along the surface normal; ρ_s is large on this surface. This will be the case for {111}. In contrast to this, if l_b is smaller along the surface normal than the surrounding orientations, ρ_s is contributed significantly by the electrons moving along the surrounding orientations also. In this case, fitting to the FS theory will give l_b averaged through the term $\exp(-d_s/l_b^k)$ over the directions around the normal. Thus, the obtained l_b should be larger than that along the sample normal. This will be the case for {110} as shown later. Here, l_b obtained by the fitting of {111} foil data to FS theory is referred to as l_b^{111}, and l_b obtained for the {110} foil is referred to as l_b^{110}. Therefore, l_b^{111} means l_b almost along ⟨111⟩ but l_b^{110} means the averaged value along the orientations around ⟨110⟩.

4.4. Anisotropy in ρ

When l_b is anisotropic, the presence of the surface brings about the anisotropy in resistivity, which does not appear on bulk specimens in the cubic system because of symmetry. This would be because σ on thin metal is composed of the summation through the term $\exp(-d_s/l_b^k)$ as seen in equation (7); in bulk specimens, this term disappears and σ is composed of the simple summation of l_b. In fact, Sato and Yonemitsu's calculation (1976) has shown the anisotropy in foil resistivity, using equation (7) for the weakly anisotropic relaxation time of the isolated Ag in Al at 4.2 K; the obtained ρ depends on the orientation relation between surface and current. Since the anisotropy in the scattering is much stronger for low-temperature phonons than the isolated Ag in Al, much stronger anisotropy in ρ_s is

expected at low temperatures in the Al of very high purity where the scattering from solutes is small. In this case, the anisotropy in ρ_s would be determined mainly by the relation between ⟨111⟩ and two orientations of surface and current, because $l_b(T)$ along ⟨111⟩ is predicted to be an order of magnitude larger than the other values as noted before.

4.5. $\rho_b l_b$ and the enhancement

As seen in subsection 4.2 (pre-analysis), the $\rho_b l_b$ obtained by the fitting of FS theory depends on the orientation. This is because the obtained l_b depends on the orientation but ρ_b does not. It should be noted that the $\rho_b l_b$ obtained is different from $\rho_b\langle l_b\rangle$, when l_b is anisotropic. Here,

$$\langle l_b\rangle = \int l_b^k \, dS_F/S_F \tag{8}$$

where the integral is taken over the Fermi surface, and S_F is the Fermi-surface area. As for $\rho_b\langle l_b\rangle$, the relation

$$(12\pi^3\hbar/e^2)/S_F = C \text{ (constant)} \tag{9}$$

holds irrespective of the anisotropy in l_b (Cotti *et al* 1964). In other words, the effect of anisotropy in l_b appears in the value of $\rho_b l_b$ on analysis with FS theory. Thus, it should be also pointed out that the size correction with FS theory will give erroneous ρ_b values if we use a constant value of $\rho_b l_b$ for single crystals with different orientations.

The theoretical value of $\rho_b\langle l_b\rangle$ can be given using the S_F calculated with a four-orthogonalized-plane-wave model on 1294 points of the Fermi surface for Al by Meador and Lawrence (1977). Their S_F is 0.79 of the free-electron value. This gives $\rho_b\langle l_b\rangle = 0.50$ fΩ m^2 (cf the free-electron value, 0.40 fΩ m^2).

In addition, in polycrystals with anisotropic l_b, Bate *et al* (1963) have shown that both ρ_s and $\rho_b l_b$ are enhanced by a factor (enhancement factor)

$$\gamma = \langle l_b^2\rangle/\langle l_b\rangle \tag{10}$$

where

$$\langle l_b^2\rangle = \int (l_b^k)^2 \, dS_F/S_F. \tag{11}$$

5. Analysis and discussion

5.1. Anisotropy in $\rho_b l_b$

To obtain the values of ρ_b, l_b and product $\rho_b l_b$, we have fitted the experimental data to equation (3) as shown in figure 6. The values obtained are listed in table 2. The slight difference in ρ_b between {111} and {110} foils is due to the error in fitting.

The values of $\rho_b l_b$ of 0.55–0.59 fΩ m^2 at 1.5 K are smaller than the previous values of 1.09 fΩ m^2 (at 1.5 K and RRR= 27 000) and 0.68 fΩ m^2 (at 4.2 K and RRR= 14 000) in Al polycrystalline foils (Nakamichi and Kino 1980, 1988), and nearer to the theoretical one of 0.50 fΩ m^2. The observation of the small $\rho_b l_b$ agrees with that on single crystals by others; Sato and Yonemitsu (1976) have obtained about 0.50–0.53 fΩ m^2 for the (101) surface

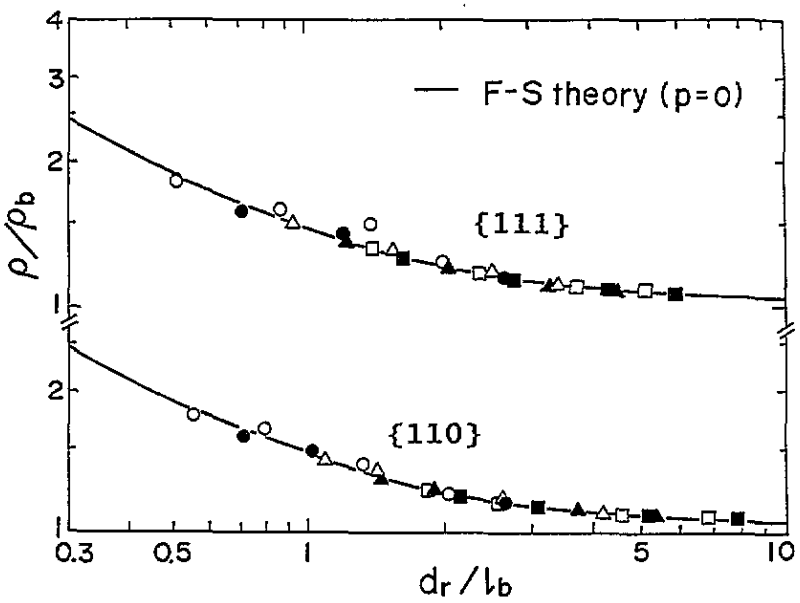

Figure 6. Two sets of data ({111} and {110}) fitted to FS theory for $p = 0$ at six different temperatures. ○, 1.5 K; ●, 10 K; △, 14 K; ▲, 16 K; □, 18 K; ■, 19 K.

Table 2. The bulk quantities ρ_b, l_b and product $\rho_b l_b$ determined by the fitting of the experimental data to FS theory for {111} and {110} foils at each temperature. $l_b(T)$ is the phonon-limited mean free path calculated from the obtained l_b, using equation (12).

	{111}				{110}			
T (K)	ρ_b (pΩ m)	l_b (μm)	$\rho_b l_b$ (fΩ m^2)	$l_b(T)$ (μm)	ρ_b (pΩ m)	l_b (μm)	$\rho_b l_b$ (fΩ m^2)	$l_b(T)$ (μm)
1.5	1.82	324	0.590		1.84	296	0.545	
10	2.68	233	0.624	1000	2.61	226	0.600	958
11	2.95	225	0.664	740	2.98	207	0.604	690
12	3.18	216	0.687	689	3.14	197	0.619	588
14	3.92	181	0.710	412	3.96	150	0.594	305
16	5.16	139	0.717	244	5.16	112	0.578	180
18	6.79	121	0.822	193	6.92	86.7	0.600	123
19	7.97	103	0.821	157	7.97	77.0	0.614	104
20				140[a]				90[a]

[a] Extrapolated value.

and current directions of [010] or [101] on Al at 4.2 K. The large $\rho_b l_b$ in polycrystals is consistent with the theoretical prediction of Bate *et al* of the enhancement of $\rho_b l_b$ in polycrystals as described in the preceding section.

Table 2 shows also that the difference in $\rho_b l_b$ between {111} and {110} foils increases with temperature. This is considered to be due to the anisotropy in electron–phonon scattering because the resistivity contribution from electron–phonon scattering rapidly increases about 10 K; it is about 30% in the total bulk resistivity at 10 K as seen in table 2. Since the impurity resistivity dominates below 10 K, the effect of anisotropy due to electron–phonon scattering on $\rho_b l_b$ is difficult to detect. However, the appreciable anisotropy in ρ_s below 10 K in figures 4 and 5(a) shows that the anisotropy in electron–phonon scattering

exists still below 10 K. Thus, the large anisotropy in $\rho_b l_b$ will come out even below 10 K, probably even at 4.2 K if a super-high-purity Al is used. The increase in $\rho_b l_b$ is large in {111} foils but small in {110} foils. This suggests that l_b^{111} differs significantly from $\langle l_b \rangle$ because of anisotropic electron–phonon scattering and l_b^{110} is near to $\langle l_b \rangle$.

5.2. *Anisotropy in l_b*

We see also from table 2 that $l_b^{111} > l_b^{110}$ as noted in subsection 4.2. The anisotropy of l_b at 1.5 K is considered to be due to the anisotropic scattering from the residual impurities in zone-refined Al. The result $l_b^{111} > l_b^{110}$ ($\rho^{111} > \rho^{110}$) at 1.5 K is consistent with the theoretical prediction regarding the residual impurities as having the scattering anisotropy of Al–Ag (Sato and Yonemitsu 1976).

The temperature-dependent part of l_b, $l_b(T)$, is calculated from the l_b values obtained using the relation

$$1/l_b(T) = 1/l_b - 1/l_b(1.5\ \mathrm{K}) \tag{12}$$

and is also listed in table 2. Figure 7 is the logarithmic plot of $l_b(T)$ against temperature T. This shows that $l_b^{111}(T)$ and $l_b^{110}(T)$ vary as $T^{-3.0}$ and $T^{-3.5}$ respectively in the range of 10–20 K. These temperature dependences of $l_b(T)$ are nearly consistent with the $T^{3.1}$ dependence of $\rho_b(T)$ shown in figure 5(*b*). In addition the $T^{3.1}$ dependence of $\rho_b(T)$ is also nearly consistent with the T^3 dependence of the scattering rate observed by a surface-Landau-level-resonance measurement at 2–20 K on Al (Doezema and Wegehaupt 1975). The T^{-3} dependence of $l_b^{111}(T)$ agrees with that of umklapp electron–phonon scattering dominating in this temperature range.

Furthermore, it should be noted that the observed $T^{-3.5}$ dependence of $l_b^{110}(T)$ is consistent with the prediction of the deviation from the T^3 power law: Meador and Lawrence's theoretical calculation (1977) has shown that, in free-electron regions between L ($\langle 111 \rangle$) and K ($\langle 110 \rangle$) on the Fermi surface, the umklapp process causes a more rapid increase than $T^{3.0}$ for temperatures above about 10 K. Similar theoretical predictions have been made by Tomlinson and Carbotte (1976) and Leung *et al* (1976).

Also, the fact $l_b^{111}(T) > l_b^{110}(T)$ is physically reasonable, because the point L corresponding to $\langle 111 \rangle$ on the Fermi surface is the furthest from the Brillouin zone boundary and has less umklapp scattering compared with $\langle 110 \rangle$. The value of $l_b^{111}(T) = 140\ \mu$m at 20 K is the same as that from the theoretical calculation of the relaxation time τ in Al by Leung *et al* (1976), where $l_b = \tau v$ and the electron velocity $v = 2.02 \times 10^6$ m s^{-1}. In addition, the value nearly agrees with that of 130 μm obtained from the extrapolation of the data measured by a Sondheimer size-effect experiment on Al at 3–11 K for the electron orbit near the L point ($\langle 111 \rangle$) in the (111) hexagonal face (Sato 1980).

The value of $l_b^{110}(T) = 90\ \mu$m at 20 K is much larger than 14 μm for that along the $\langle 110 \rangle$ direction by the calculation of Leung *et al* (1976). In contrast to that around the $\langle 111 \rangle$ direction, l_b around the $\langle 110 \rangle$ direction sharply increases on deviation from $\langle 110 \rangle$ towards $\langle 111 \rangle$ on the Fermi surface (Leung *et al* 1977). Thus, the electrons moving in such a direction, deviating from $\langle 110 \rangle$, may have a considerable contribution to ρ_s. This must have given the larger l_b value as described in subsection 4.3.

Now, over the wider temperature range, let us deduce the information on anisotropy in l_b using figure 4. l_b at 1.5 K is about 310 μm according to table 2, and the condition of $l_b < 2d_r$ for the use of equation (5) is satisfied for 160 μm thickness over the whole temperature range measured. From equations (5) and (9), we obtain

$$\rho^{111} - \rho^{110} = (0.46C/d_r)(l_b^{111} - l_b^{110})/\langle l_b \rangle. \tag{13}$$

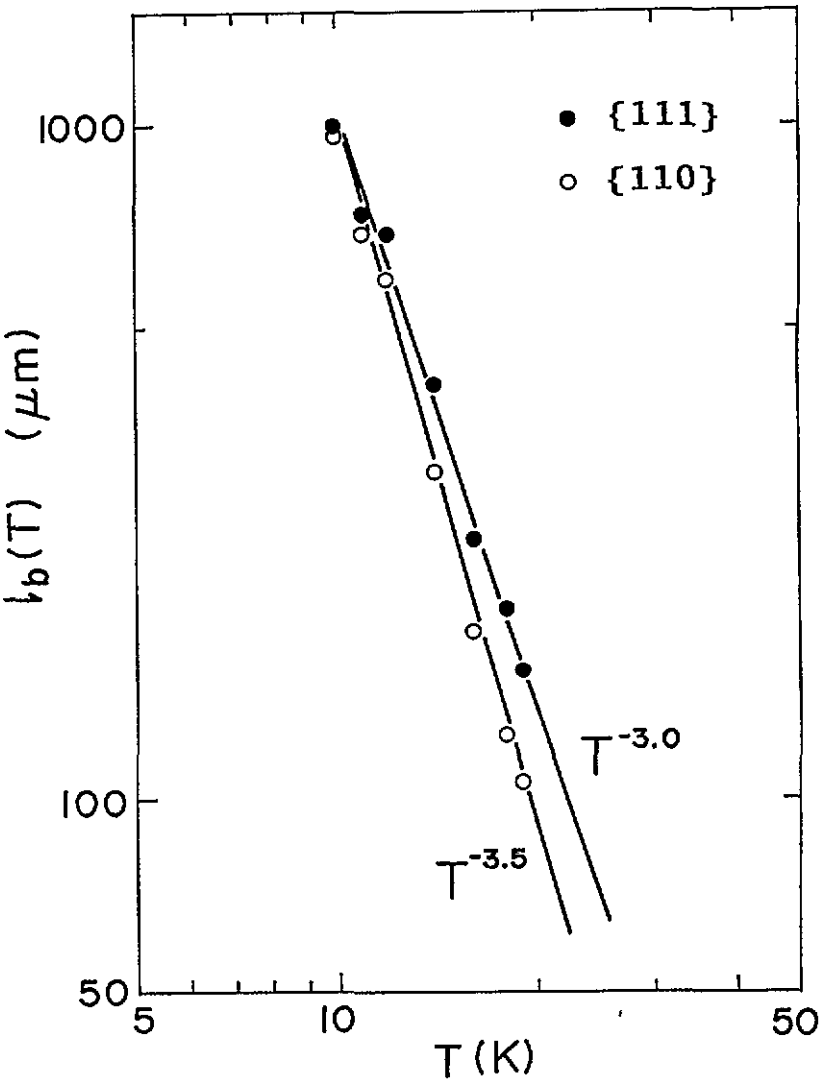

Figure 7. The logarithmic plot of the phonon-limited part of the bulk mean free path $l_b(T)$ against T, where the data in table 2 are used. ●, $l_b(T)$ on {111} foils ($l_b^{111}(T)$); ○, $l_b(T)$ on {110} foils ($l_b^{110}(T)$). These correspond to $l_b(T)$ along ⟨111⟩ and that along the orientations around ⟨110⟩, respectively.

We define the anisotropic factor f_{an} between l_b along about ⟨111⟩ and ⟨110⟩ as

$$f_{an} = (l_b^{111} - l_b^{110})/\langle l_b \rangle \tag{14}$$

i.e. the relative difference between l_b^{111} and l_b^{110}. Using equation (13), this is converted to

$$f_{an} = (d_r/0.46C)(\rho^{111} - \rho^{110}). \tag{15}$$

f_{an} defined by equation (14) is rather smaller than the relative difference of l_b between the two points for ⟨111⟩ and ⟨110⟩ on the Fermi surface, because l_b^{110} is rather larger than

l_b along just ⟨110⟩ as described above. However, this can give the feature of temperature dependence of the anisotropy in l_b. Thus, we calculate f_{an} with equation (15) using the values of $\rho^{111} - \rho^{110}$ for 163 and 169 μm thicknesses in figure 4. For the value of C, the theoretical value equal to 0.50 fΩ m^2 is taken, because the experimental value may be affected by anisotropic scattering.

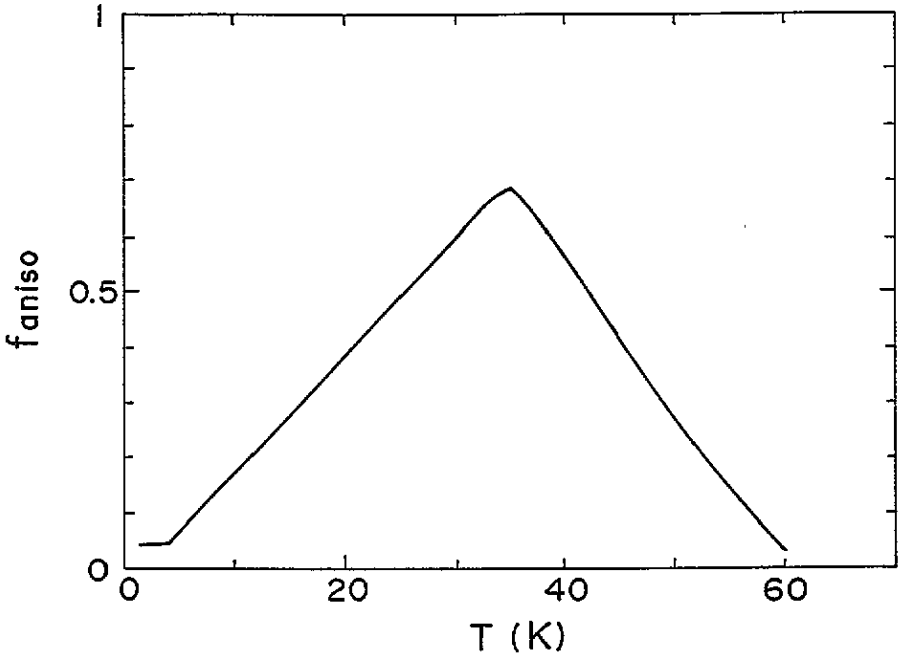

Figure 8. The temperature dependence of the anisotropy factor, $f_{an} = (l_b^{111} - l_b^{110})/\langle l_b \rangle$, obtained from the present experiment. $\langle l_b \rangle$ is l_b averaged over the Fermi surface (for the meaning of l_b^{111} and l_b^{110}, see the caption of figure 7).

The f_{an} obtained is shown in figure 8. f_{an} increases with T and has the maximum value of 0.72 at about 35 K, then decreases with T. Taking $\langle l_b \rangle$ to be equal to l_b^{110} as suggested in subsection 5.1, we obtain $l_b^{111}/l_b^{110} = f_{an} + 1$. This suggests that the ratio l_b^{111}/l_b^{110} also shows a temperature dependence similar to that of f_{an}. The feature of temperature dependence of the anisotropy obtained is consistent with the result of Leung *et al* (1977), who have calculated the relaxation time at 20, 50 and 100 K and shown that the anisotropy is very large at 20 K, becoming small at 50 K and even smaller at 100 K.

5.3. The magnitude of ρ_s

It is interesting to compare ρ_s in different systems. Figure 9 is ρ_s in four different systems plotted against ρ_b for foils with nearly the same thicknesses. The nature of bulk scattering divides them in two: impurity dominated (Al–Ag at 4.2 K) and phonon dominated (pure Al at low temperatures). The latter is further divided into polycrystal and single crystal. For single-crystal data, ρ_s is obtained as the subtraction of ρ_b from the measured ρ, using ρ_b in table 2. The foil data on the Al–Ag polycrystal and pure Al polycrystal with RRR= 27 000 are from our previous work (Nakamichi and Kino 1980, 1988). The theoretical ρ_s is

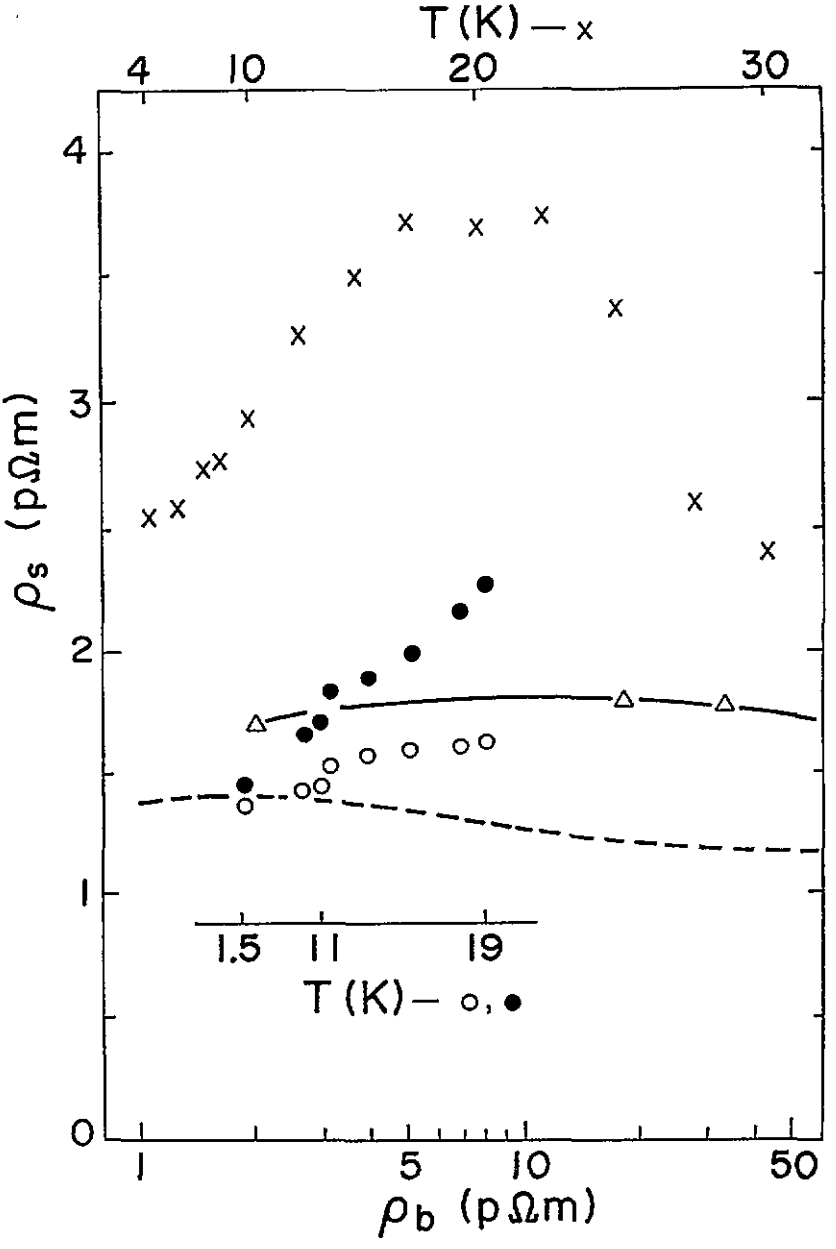

Figure 9. The surface resistivity ρ_s plotted against ρ_b for foils with nearly the same thicknesses in various systems, where ρ_b obtained from the fitting of the data to FS theory is used. ×, a polycrystalline Al foil of 184 μm thickness; ●, a {111} Al foil of 169 μm; ○, a {110} Al foil of 163 μm; △, a polycrystalline Al–Ag foil of 189 μm at 4.2 K. The dashed line is the theoretical one from FS theory, where $\rho_b l_b = 0.50$ fΩ m^2 is used. The temperature for the Al polycrystal is shown at the top of the figure and that for Al single crystals is beside the data.

calculated by equation (6), using the $\rho_b l_b$ value equal to 0.50 fΩ m^2, and shown by the broken line.

We see that ρ_s in the polycrystal of pure Al is about twice as large as the others. ρ_s in polycrystalline Al–Ag, which has nearly isotropic scattering, hardly varies with ρ_b. ρ_s in single crystals of pure Al is a little smaller below 12 K than that in Al–Ag. However, above 12 K, ρ_s^{111} for pure Al becomes larger than ρ_s for Al–Ag. Since the resistivity due to electron–phonon scattering becomes over 40% in the total resistivity above 12 K according to table 2, this must be due to the anisotropy in $l_b(T)$ ($l_b(T)^{111} > l_b(T)^{110}$). These features are more clearly seen in figure 5(*a*), where the same specimens as in figure 9 is used for pure Al. As described in section 3, $\rho_s(T)$ in polycrystals is about twice as large as that of the single crystal with {111}; in addition, $\rho_s^{111}(T)$ is about three times as large as ρ_s^{110} below about 14 K. These facts show that the large enhancement of ρ_s in Al polycrystals strongly correlates with the anisotropic electron–phonon scattering.

This enhancement of ρ_s is consistent with the theoretical prediction of Bate *et al* (1963), similar to the case of $\rho_b l_b$ described in subsections 4.2 and 5.1. The enhancement factor γ defined by equation (10) has been theoretically calculated to be 1.15 for Al–Ag at 4.2 K by Sato and Yonemitsu (1976). This means a small enhancement of the Al–Ag polycrystalline system and is consistent with figure 8. In contrast to this, the γ for the pure Al polycrystal at low temperatures must be much larger, because the relaxation time due to electron-phonon scattering at low temperatures has been shown to vary by more than a factor of 10 over the Fermi surface both theoretically (Leung *et al* 1976, 1977) and experimentally (Wegehaupt and Doezema 1978). In addition, as shown in subsection 5.2, the anisotropy in l_b due to electron–phonon scattering is large at 10–60 K, maximizing at around 35 K between l_b^{111} and l_b^{110}. This temperature range is consistent with the range where the large discrepancy in ρ_s has been observed between FS theory and experiments (see the review by Bass (1972)).

6. Summary and conclusions

A temperature-dependent anisotropy in the surface resistivity ρ_s is found between {111} and {110} foils in the ⟨112⟩ current direction at 1.5–60 K. Both FS and Soffer's theories show that this does not arise from the difference between the surface-reflection parameters.

The bulk mean free path l_b obtained from the fitting of the experimental data to FS theory has shown anisotropy. The phonon-limited part of l_b agrees with theoretical predictions of anisotropic electron–phonon relaxation time, in both its magnitude (along about ⟨111⟩ at 20 K) and the n values of T^n dependence (at 10–20 K).

The product $\rho_b l_b$ obtained depends on both orientation and temperature. It is pointed out that $\rho_b l_b$ differs from $\rho_b(l_b)$(= constant), and that the size correction with FS theory will give erroneous ρ_b values if a constant $\rho_b l_b$ value is used for the single crystals with anisotropic l_b.

The difference in resistivity between {111} and {110} foils shows that the relative difference in l_b between directions along about ⟨111⟩ and ⟨110⟩ is large at 10–60 K, maximizing at about 35 K. Moreover, ρ_s is found to be about twice as large in a polycrystalline foil than a single-crystal one in pure Al below a few tens of kelvin; in addition, $\rho_s^{111}(T)$ is observed to be about three times as large as $\rho_s^{110}(T)$ below about 14 K.

In contrast to these foils dominated by anisotropic electron-phonon scattering, ρ_s does not significantly depend on ρ_b (or l_b) in Al–Ag foil at 4.2 K, where the bulk scattering is nearly isotropic. These facts are qualitatively consistent with the anisotropy enhancement theory of Bate *et al*.

It is thus concluded that the discrepancy between FS theory and measured ρ_s in the previous measurement mainly arises from the enhancement of ρ_s due to the anisotropic electron–phonon scattering in Al polycrystals.

Acknowledgment

I would like to thank Professor Takao Kino for introducing me to this size-effect experiment and for his encouragement.

References

Bass J 1972 *Adv. Phys.* **21** 431–604
Bate R T, Byron M and Hille P F 1963 *Phys. Rev.* **131** 1482–8
Chambers R G 1969 *The Physics of Metals–1: Electrons* ed Ziman (Cambridge: Cambridge University Press) pp 175–89
Cotti P, Fryer E M and Olsen J L 1964 *Helv. Phys. Acta* **37** 585–8
Dingle R B 1950 *Proc. R. Soc.* A **201** 545–60
Doezema R E and Wegehaupt T 1975 *Solid State Commun.* **17** 631–4
Fuchs K 1938 *Proc. Camb. Phil. Soc.* **34** 100–8
Kawata S and Kino T 1975 *J. Phys. Soc. Japan* **39** 684–91
Kirkland L R and Chaplin R L 1971 *J. Appl. Phys.* **42** 3054–7
Leung H K, Carbotte J P, Taylor D W and Leavens C R 1976 *Can. J. Phys.* **54** 1585–99
Leung H K, Kus F W, Mackay N and Carbotte J P 1977 *Phys. Rev.* B **16** 4358–64
Meador A B and Lawrence W E 1977 *Phys. Rev.* B **15** 1850–8
Nakamichi I 1989 *J. Phys.: Condens. Matter* **1** 8887–99
Nakamichi I and Kino T 1980 *J. Phys. Soc. Japan* **49** 1950–7
—— 1988 *J. Phys. F: Met. Phys.* **18** 2421–8
Parsons D and Steele C A 1979 *J. Phys. F: Met. Phys.* **9** 1783–96
Risnes R 1970 *Phil. Mag.* **21** 591–7
Risnes R and Sollien V 1969 *Phil. Mag.* **20** 895–905
Sambles J R and Elson K C 1980 *J. Phys. F: Met. Phys.* **10** 1487–94
Sambles J R and Munday J N 1983 *J. Phys. F: Met. Phys.* **13** 2281–92
Sambles J R and Preist T W 1982 *J. Phys. F: Met. Phys.* **12** 1971–87
Sato H 1980 *J. Low Temp. Phys.* **38** 267–75
Sato H and Yonemitsu K 1976 *Phys. Status Solidi* b **73** 725–33
Soffer S B 1967 *J. Appl. Phys.* **38** 1710–5
Sondheimer E H 1952 *Adv. Phys.* **1** 1–42
Tomlinson P G and Carbotte J P 1976 *Solid State Commun.* **18** 119–22
Wegehaupt T and Doezema R E 1978 *Phys. Rev.* B **18** 742–8